Cascade calculation of hadronic hydrogen atoms

T. P. Terada and R. S. Hayano
Department of Physics, School of Science, University of Tokyo, 7-3-1 Hongo, Bunkyo-ku, Tokyo 113, Japan
(Received 17 July 1996)

Cascade calculations of hadronic hydrogen atoms are performed to obtain the x-ray yields as a function of the target density. An extension of Leon-Bethe's Stark mixing rates to $m \neq 0$ states is made without the introduction of the parameter k_{STK}, which is necessary in the Borie-Leon model to enhance the Stark mixing rates. Although the energies of their L x rays are too low to observe, we can roughly estimate the $2p$ absorption width of pionic and kaonic hydrogen atoms from the measured K x-ray yields. [S0556-2813(97)03601-7]

PACS number(s): 36.10.−k, 13.75.−n, 25.43.+t, 25.80.−e

I. INTRODUCTION

Hadronic hydrogen atoms are of particular interest among hadronic atoms because they have the simplest structure and are free from any screening effects due to bound electrons. We can directly probe hadron-nucleon interaction at zero energy in these systems, but unfortunately the x-ray yields are specifically small compared to other hadronic atoms with $Z \geqslant 2$ because of Stark mixing as Day *et al.* [1,2] first indicated. Since it is electrically neutral, small in size and has no electron, the hadronic hydrogen atom passes freely near the neighboring hydrogen atom, where it will be subjected to a strong electric field of the proton. This induces the Stark mixing between the states of different angular momentum and consequently the hadron is absorbed by the nucleus from low angular momentum states at a high principle quantum number n before the hadronic atom can deexcite to reach low-lying n states by radiative transitions which we can observe. The resultant x-ray yields are very low particularly for liquid hydrogen targets, where the density is high and the probability of these collisions is enhanced.

The first calculation of hadronic hydrogen atoms with the Stark effect included was made by Leon and Bethe [3] for liquid hydrogen target. Borie and Leon [4] made a more detailed cascade calculation to obtain the target density dependence of the x-ray yields, assuming that the rates of Stark mixing to neighboring angular momentum eigenstates are given by Leon-Bethe's prescription. Although the Borie-Leon model has often been used to explain the later experimental data of x-ray yields from hadronic hydrogen atoms, it always requires an additional free parameter k_{STK} of 1.5 to 2.0 to enhance the Stark mixing rate [5]. This has been attributed to some approximations made in Leon and Bethe's calculation, but no satisfactory explanation was given so far.

In this paper, a more realistic description of Stark mixing rates is formulated on the basis of Leon and Bethe's model and applicated to Borie and Leon's cascade calculation in the aim of eliminating the factor of k_{STK}. The results are compared with the very recent series of data on the density dependence of x-ray yields from antiprotonic and pionic hydrogen atoms, and the model is then applied to kaonic hydrogen atoms on which very little is known.

II. CASCADE MODEL OF EXOTIC HYDROGEN ATOMS

A. Atomic cascade

The incident hadron loses energy by ionization of target hydrogen molecules and collision with electrons of comparable velocities until it is captured to form an exotic hydrogen atom. We only have an incomplete and qualitative understanding of these processes, but this is not so crucial to calculation on the atomic cascade after the capture. Since the dissociation energy of hydrogen molecules is 4.7 eV, the hadronic atom is expected to have a kinetic energy of about 1 eV at the end of these molecular processes.

The captured hadron is initially in an orbit with the principal quantum number $n \sim \sqrt{\mu}$ where μ is the reduced mass of the hadron-hydrogen system, because the Bohr radius corresponds to that of the K-shell electrons and thus the overlap of the wave functions of the hadronic atom and ground state hydrogen is the largest. In most of the calculations the initial population distribution at $n \sim \sqrt{\mu}$ is taken to be statistical: $P(l) \propto (2l+1)$. In the case of hadronic hydrogen atoms, the Stark mixing rate is high enough to level off the population of different angular momentum states so that x-ray yields at low-lying n states are not affected by the initial population distribution as will be shown later.

The atomic cascade involves successive deexcitation processes through the atomic states to states with smaller n until the hadron is captured by the nucleus through strong interaction from low angular momentum states. Figure 1 illustrates the atomic cascade processes diagrammatically. More detailed description on these processes are to be found in some review papers such as Ref. [6].

B. Cascade calculation

The method of cascade calculation used in the present paper is a standard one by Borie and Leon [4] except for the Stark mixing rates. We summarize the physical processes in the atomic cascade and introduce the arrival probability, and then describe the procedure of the calculation.

1. Processes included in the cascade calculation

a. Molecular dissociation. Initially at states with large n the hadronic hydrogen atom deexcites by dissociation of the neighboring hydrogen molecules, but this process is less im-

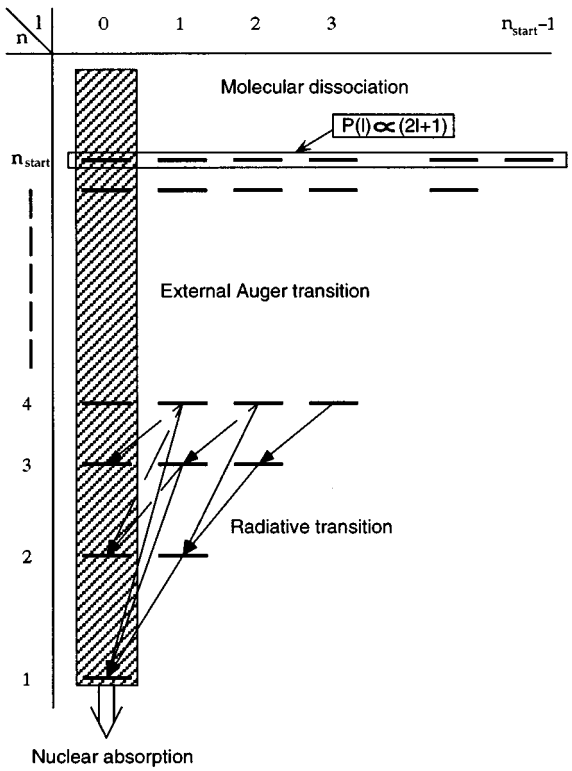

FIG. 1. A schematic level diagram of an exotic atom showing some of the possible deexcitation processes.

portant at states with small n such as $n \leqslant \sqrt{\mu}$. Thus we merely assume that the cross section is given by the size of the hadronic hydrogen atom:

$$\Gamma^{\rm mol}_{n,l\to n',l} = \frac{N}{2} v \pi r_n^2, \tag{1}$$

where n' is the largest of which satisfy $\Delta E_{n\to n'} \geqslant 4.7$ eV (the dissociation energy of hydrogen molecule), N is the target density of hydrogen atoms ($N/2$ is that of hydrogen molecules), v is the velocity of the hadronic hydrogen atom, and r_n is Bohr radius of the hadronic hydrogen atom in nth Bohr orbit.

b. External Auger transition. The external Auger deexcitation, which involves ionization of the neighboring hydrogen molecules, becomes important at $n \sim \sqrt{\mu}$. Leon and Bethe [3] showed that the rate is given approximately by

$$\Gamma^{\rm Auger}_{n,l\to n',l'} \simeq \frac{16}{3}\pi \frac{N}{\mu^2} \frac{\max(l,l')}{2l+1} \times |\langle n',l'\|r\|n,l\rangle|^2 (2\Delta E_{\rm released} + 1.39)^{-1/2}, \tag{2}$$

where $l' = l \pm 1$, $\langle n',l'\|r\|n,l\rangle$ is the radial dipole matrix element for the transition of a hydrogenlike atom given in Ref. [7] and $\Delta E_{\rm released}$ is $\Delta E_{n\to n'} - 15.2$ eV (the ionization energy of hydrogen molecule).

c. Radiative transition. Radiative transitions, involving the emissions of x rays, dominate at low n states. The rates are given by

$$\Gamma^{\rm rad}_{n,l\to n',l'} = \frac{4}{3}\frac{\alpha}{\mu^2}\frac{\max(l,l')}{2l+1} |\langle n',l'\|r\|n,l\rangle|^2 (\Delta E_{n\to n'})^3, \tag{3}$$

where α is the fine structure constant.

d. Nuclear absorption. The rates for nuclear absorption scale as

$$\Gamma^{\rm nuclear}_{ns} = \frac{\Gamma^{\rm nuclear}_{1s}}{n^3}, \tag{4}$$

$$\Gamma^{\rm nuclear}_{np} = \frac{32}{3}\frac{n^2-1}{n^5}\Gamma^{\rm nuclear}_{2p}, \tag{5}$$

where $\Gamma^{\rm nuclear}_{1s}$ and $\Gamma^{\rm nuclear}_{2p}$ are mainly taken from the experimental results. $\Gamma^{\rm nuclear}_{ns}$ also suppresses the Stark mixing as will be described.

e. Weak decay. Except for the antiprotonic hydrogen atom, weak decay of the orbiting particle plays a role when the target gas is dilute. The rate is given by

$$\Gamma^{\rm weak} = \frac{1}{\tau}, \tag{6}$$

where τ is the mean life of the particle.

f. Stark mixing. Stark mixing rates $\Gamma^{\rm Stark}_{n,l\to n,l'}$ will be described in detail in the following sections.

2. Arrival probability

When a hadronic atom cascades down through many states of $|n,l\rangle$ as displayed in Fig. 1, the deexcitation processes and the Stark mixings are the competing processes. The population distribution $P_{n,l}$ satisfies the following rate equation:

$$\frac{dP_{n,l}}{dt} = -\Gamma^{\rm total}_{n,l} P_{n,l} + \sum_{l'\neq l} \Gamma^{\rm Stark}_{n,l'\to n,l} P_{n,l'}, \tag{7}$$

where

$$\Gamma^{\rm total}_{n,l} = \sum_{n'<n} (\Gamma^{\rm mol}_{n,l\to n',l'} + \Gamma^{\rm Auger}_{n,l\to n',l'} + \Gamma^{\rm rad}_{n,l\to n',l'}) + \Gamma^{\rm nuclear}_{n,l} + \Gamma^{\rm weak} + \sum_{l'\neq l} \Gamma^{\rm Stark}_{n,l\to n,l'}. \tag{8}$$

We define

$$\widetilde{P}_{n,l} = \Gamma^{\rm total}_{n,l} \int_0^\infty P_{n,l} dt, \tag{9}$$

which is the *arrival probability*: the overall population which goes out from a state $|n,l\rangle$ to elsewhere. Integrating Eq. (7) and assuming $P_{n,l}(t=+\infty)=0$, we obtain

$$P_{n,l}(t=0) = \widetilde{P}_{n,l} - \sum_{l'\neq l} \frac{\Gamma^{\rm Stark}_{n,l'\to n,l}}{\Gamma^{\rm total}_{n,l'}} \widetilde{P}_{n,l'}. \tag{10}$$

Equation (10) can be expressed in the form of a matrix equation

$$\begin{pmatrix} P_{n,l=0}(t=0) \\ P_{n,l=1}(t=0) \\ \vdots \\ P_{n,l=n-1}(t=0) \end{pmatrix} = \begin{pmatrix} 1 & -\frac{\Gamma^{\text{Stark}}_{n,l=1\to n,l=0}}{\Gamma^{\text{total}}_{n,l=1}} & \cdots & -\frac{\Gamma^{\text{Stark}}_{n,l=n-1\to n,l=0}}{\Gamma^{\text{total}}_{n,l=n-1}} \\ -\frac{\Gamma^{\text{Stark}}_{n,l=0\to n,l=1}}{\Gamma^{\text{total}}_{n,l=0}} & 1 & \ddots & \vdots \\ \vdots & \ddots & \ddots & -\frac{\Gamma^{\text{Stark}}_{n,l=n-1\to n,l=n-2}}{\Gamma^{\text{total}}_{n,l=n-1}} \\ -\frac{\Gamma^{\text{Stark}}_{n,l=0\to n,l=n-1}}{\Gamma^{\text{total}}_{n,l=0}} & \cdots & -\frac{\Gamma^{\text{Stark}}_{n,l=n-2\to n,l=n-1}}{\Gamma^{\text{total}}_{n,l=n-2}} & 1 \end{pmatrix} \times \begin{pmatrix} \widetilde{P}_{n,l=0} \\ \widetilde{P}_{n,l=1} \\ \vdots \\ \widetilde{P}_{n,l=n-1} \end{pmatrix} \tag{11}$$

and solved by standard methods for matrix inversion.

3. Procedure of the cascade calculation

Cascade calculation for a set of parameters (mass of the orbiting particle, initial kinetic energy of the hadronic hydrogen atom, target density and $1s$ state shift and width by the nuclear absorption) is performed in the following way (see again Fig. 1).

(1) The initial population at $n\sim\sqrt{\mu}$ is given by a statistical distribution $P_{n,l}(t=0)\propto(2l+1)$.

(2) Solve Eq. (11) to obtain the arrival probability $\widetilde{P}_{n,l}=\Gamma^{\text{total}}_{n,l}\int_0^\infty P_{n,l}dt$.

(3) Distribute $\widetilde{P}_{n,l}$ to lower-n states or other processes according to $\Gamma^{\text{process}}_{n,l\to\text{somewhere}}/\Gamma^{\text{total}}_{n,l}$ and sum up the radiative transition rates.

(4) Reduce n by 1.

(5) Repeat (2) to (4) until $n=2$.

C. Stark mixing of degenerate states

When the small and electrically neutral hadronic hydrogen atom passes through the electric field inside the electron cloud of the target hydrogen atoms, Stark mixings among the n^2 degenerate states are induced. We calculate the Stark mixing rates by extending Leon-Bethe's calculation [3], which is for transitions among $m=0$ states, to those among $m\neq0$ states, and avarage them over initial $2l+1$ substates as in Borie-Leon model [4].

1. Impact parameter method

As there is enough time during a collision for the atom to make many transitions among the states, the Born approximation is not applicable. Instead we use the *impact parameter method* as in Ref. [3] with the following two assumptions: (i) The density distribution of electronic cloud is not affected by the presence of the hadronic atom because it is electrically neutral. (ii) The hadronic atom passes a definite and straight trajectory through the fixed electronic cloud. This is justified by the velocity of the hadronic atom $v\sim10^4$ m/sec, which is five times as large as the thermal velocity of a hydrogen molecule $v_{\text{thermal}}=\sqrt{3kT/m_{\text{H}_2}}\sim2\times10^3$ m/sec (at $T=$ 300 K). We calculate the Stark mixing rates as a function of impact parameter in this approximation, taking into account transitions among the degenerate states but ignoring much less likely transitions to states with different n.

2. Fixed field model

We start with the time-dependent Schrödinger equation for the internal coordinate of the hadronic atom

$$i\frac{\partial}{\partial t}|\psi(t)\rangle=H(t)|\psi(t)\rangle \tag{12}$$

with

$$H(t)=H_0+V(t),\quad V(t)=\mathbf{E}\cdot\mathbf{r}, \tag{13}$$

where H_0 is the operator of the unperturbed energy of the hadronic atom, which contains the strong interaction shift as well as the electromagnetic energy, $\mathbf{E}$ the shielded electric field by a hydrogen atom, and $\mathbf{r}$ the internal coordinate of the hadronic hydrogen atom. Expanding the wave function $|\psi(t)\rangle$ into an orthonormal set of n^2 eigenfunctions $|\alpha\rangle$ (all having the same n), multiplying $\langle\beta|$ from the left-hand side and taking the coordinate system as shown in Fig. 2, we obtain in the interaction representation

$$\begin{aligned} i\frac{\partial}{\partial t}\langle\beta|\psi(t)\rangle &= \sum_\alpha\left[\langle\beta|V(t)|\alpha\rangle - i\langle\beta|\frac{\partial}{\partial t}|\alpha\rangle\right]\langle\alpha|\psi(t)\rangle \\ &= \sum_\alpha\left[E(t)\langle\beta|z|\alpha\rangle - i\,\dot\theta\langle\beta|\frac{\partial}{\partial\theta}|\alpha\rangle\right]\langle\alpha|\psi(t)\rangle, \end{aligned} \tag{14}$$

where $E(t)$ is the electric field strength. Reifenröther and Klempt [8,9] solved this set of simultaneous differential equations numerically using the spherical harmonics $|l,m\rangle$ as their orthonormal set, but their calculation entails a heavy

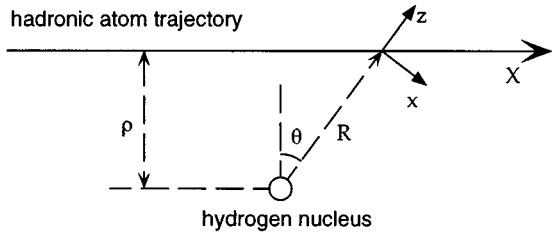

FIG. 2. The coordinate system for the Stark mixing calculation: z axis is in the electric field direction, x axis in the plane of collision, and θ the angle between x axis and the direction of the motion. $R=\rho\sec\theta$, $X=\rho\tan\theta$, $dX=v\,dt=\rho\sec^2\theta\,d\theta$.

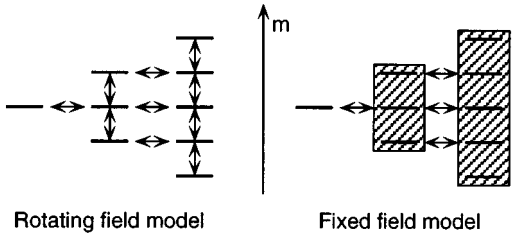

FIG. 3. Difference between the rotating field model and the fixed field model. In Eq. (14), $\langle\beta|z|\alpha\rangle$ are the Stark induced transitions with $\Delta l=\pm1$, $\Delta m=0$, and $\langle\beta|\partial/\partial\theta|\alpha\rangle=i\langle\beta|L_y|\alpha\rangle$ are the transitions by the rotation of the quantization axis with $\Delta l=0$, $\Delta m=\pm1$.

task because all populations in n^2 states of a given n are calculated at every integration step.

On the other hand, Eq. (14) is greatly simplified by omitting the $\dot\theta$ terms because the Stark interaction $V=\mathbf{E}\cdot\mathbf{r}$ is diagonal when we expand the wave function $|\psi(t)\rangle$ with the eigenfunctions in the parabolic coordinate $|n_1,m\rangle$ instead of spherical harmonics $|l,m\rangle$. Since the $\dot\theta$ terms arise from the rotation of the axis of quantization (i.e., z axis) during the collision processes, the angular momentum m is fixed in the field direction in this model. We call Eq. (14) the *rotating field model* and dropping $\dot\theta$ terms yields the *fixed field model* [3]. We also assume a uniform population distribution in $2l+1$ substates of a given l and take into account only the transitions between states with different l, as schematically shown in Fig. 3.

We can separate Eq. (14) to a set of differential equations for $\langle n_1,m|\psi(t)\rangle$ in the fixed field model as follows:

$$i\frac{\partial}{\partial t}\langle n_1,m|\psi(t)\rangle=\sum_{n_1'}\langle n_1,m|V(t)|n_1',m\rangle\langle n_1',m|\psi(t)\rangle$$
$$=V_{n_1,m}(t)\langle n_1,m|\psi(t)\rangle, \tag{15}$$

where

$$V_{n_1,m}(t)=\frac{3}{2}E(t)n(n_1-n_2)=\frac{3}{2}E(t)n(2n_1-n+|m|+1). \tag{16}$$

n_1 and n_2 are the parabolic quantum numbers which satisfy $n_1+n_2+|m|+1=n$. The screened electric field strength at a distance of R from a hydrogen atom in its ground state is

$$E(R)=\frac{Z_{\rm eff}}{\mu R^2}=\left(1-\int_0^R|R_{n=1,l=0}|^2r^2dr\right)\frac{1}{\mu R^2}$$
$$=e^{-2R}\frac{1+2R+2R^2}{\mu R^2}, \tag{17}$$

where $Z_{\rm eff}$ is the effective nuclear charge of the hydrogen atom (<1) and $R_{n=1,l=0}=2e^{-R}$ the radial wave function for an electron of hydrogen atom in its ground state. Integrating Eq. (15), we have

$$\langle n_1,m|\psi(t)\rangle=\langle n_1,m|\psi(t=-\infty)\rangle$$
$$\times\exp\left[-i\int_{-\infty}^{t}V_{n_1,m}(t')dt'\right]. \tag{18}$$

Putting $|\psi(t=\infty)\rangle=|l,m\rangle$ and $|\psi(t=-\infty)\rangle=|l',m\rangle$, the total transition probability for $|l,m\rangle\to|l',m\rangle$ over a continuous interaction with a hydrogen atom along a straight-line path with an impact parameter ρ is obtained as

$$P(\rho,l,l';m)=\left|\sum_{n_1=0}^{n-|m|-1}\langle l,m|n_1,m\rangle\exp\left[-i\int_{-\infty}^{\infty}V_{n_1,m}(t)dt\right]\langle n_1,m|l',m\rangle\right|^2$$
$$=\left|\sum_{n_1=0}^{n-|m|-1}\langle l,m|n_1,m\rangle\exp\left[-i\frac{3}{2}\pi\frac{n(2n_1-n+|m|+1)}{v\mu}\frac{\zeta(\rho)}{\rho}\right]\langle n_1,m|l',m\rangle\right|^2$$
$$=\left|\sum_{n_1=0}^{n-|m|-1}\langle l,m|n_1,m\rangle\exp\left[-in_1\frac{3\pi n}{v\mu}\frac{\zeta(\rho)}{\rho}\right]\langle n_1,m|l',m\rangle\right|^2, \tag{19}$$

where we have used Leon-Bethe's $\zeta(\rho)$ [3]

$$\zeta(\rho)=\frac{1}{\pi}\int_{-\pi/2}^{\pi/2}e^{-2\rho\sec\theta}(1+2\rho\sec\theta+2\rho^2\sec^2\theta)d\theta \tag{20}$$

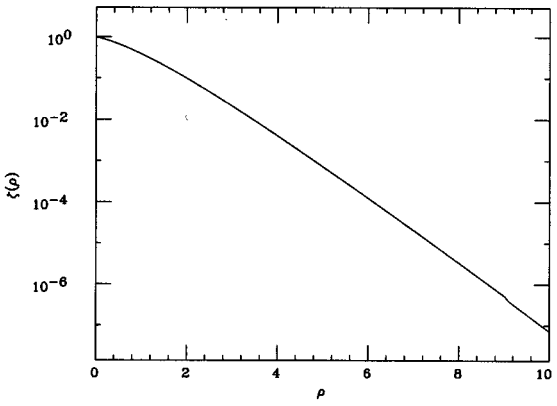

FIG. 4. $\zeta(\rho)$ as a function of ρ.

and its variation as a function of ρ is shown in Fig. 4. The coefficients $\langle l,m|n_1,m\rangle$ can be obtained by a method given in the appendix of Ref. [3]. In this picture, each of the Stark eigenstates $|n_1,m\rangle$ interferes with the others at $t=\infty$ with its own accumulated phase $\int_{-\infty}^{\infty}V_{n_1,m}(t)dt$ (see Fig. 5). Note that $\Delta l\geqslant 2$ transitions are possible as results of multiple interactions, and that $\Delta m=0$ transition is prohibited.

3. Stark mixing rates in the present model

The Stark mixing rates for the transitions $|n,l\rangle\rightarrow|n,l'\rangle$ (averaged over initial substates) are obtained as

$$\Gamma^{\text{Stark}}_{l\rightarrow l'}=\frac{1}{2l+1}\sum_m \Gamma^{\text{Stark}}_{l\rightarrow l';m}$$

$$=Nv\frac{1}{2l+1}\sum_m 2\pi\int_0^{\infty}\rho d\rho P(\rho,l,l';m), \quad (21)$$

where m changes within the range $-\min(l,l')\leqslant m\leqslant\min(l,l')$ because of the selection rule $\Delta m=0$. Integrals are numerically performed with no approximation except for the assumption of impact parameter method and fixed field model, and thus this calculation fully incorporates the l, Δl and m dependence of the Stark mixing rate (see also Fig. 6).

A part of the results as an example is summarized in Table I, which is for a pionic hydrogen of kinetic energy

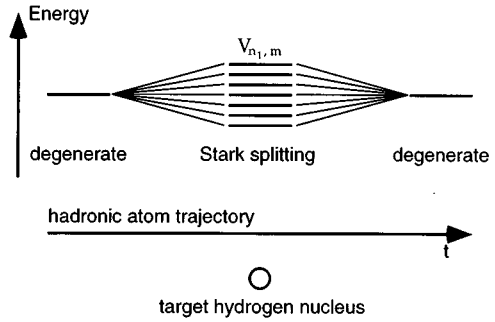

FIG. 5. Each Stark eigenstate interferes with the others at $t=\infty$ with its own accumulated phase $-i\int_{-\infty}^{\infty}V_{n_1,m}(t')dt'$.

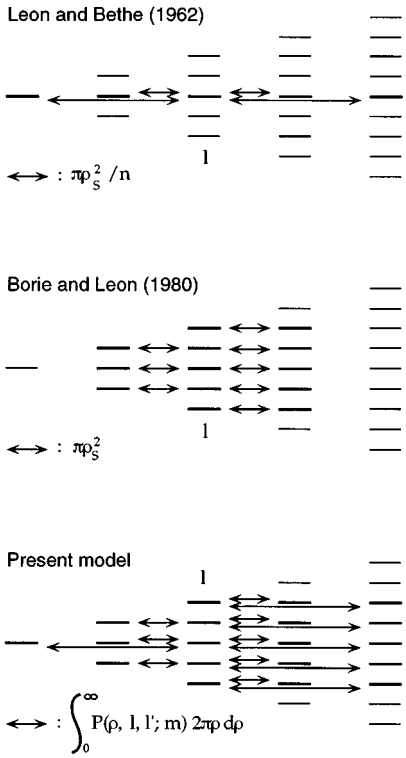

FIG. 6. Comparison of Stark mixing rates in three models: Leon-Bethe considered only transitions between $m=0$ states, Borie-Leon only $\Delta l=\pm 1$ transitions, and the present model involves all possible transitions with $\Delta m=0$.

$T=1$ eV and $n=5$. To eliminate the density dependence, the total cross section for Stark transition of $l\rightarrow l'$, namely

$$\sigma^{\text{Stark}}_{l\rightarrow l'}=\frac{\Gamma^{\text{Stark}}_{l\rightarrow l'}}{Nv} \quad (22)$$

TABLE I. Stark mixing cross sections $\sigma^{\text{Stark}}_{l\rightarrow l'}$ for pionic hydrogens in $n=5$ ($T=1.0$ eV).

(a) $\Delta l=1$ transitions for different initial l

Model		$0\rightarrow 1$	$1\rightarrow 2$	$2\rightarrow 3$	$3\rightarrow 4$
Borie-Leon model $\pi\rho_S^2$		16.3	16.3	16.3	16.3
Present model	$m=3$				9.92
	$m=2$			7.42	5.56
	$m=1$		7.02	7.20	5.73
	$m=0$	7.89	6.72	4.50	5.30

(b) Transitions with different Δl for a given final l

Model		$0\rightarrow 4$	$1\rightarrow 4$	$2\rightarrow 4$	$3\rightarrow 4$
Borie-Leon model $\pi\rho_S^2$					16.3
Present model	$m=3$				9.92
	$m=2$			6.54	5.56
	$m=1$		4.91	2.56	5.73
	$m=0$	3.37	1.10	3.69	5.30

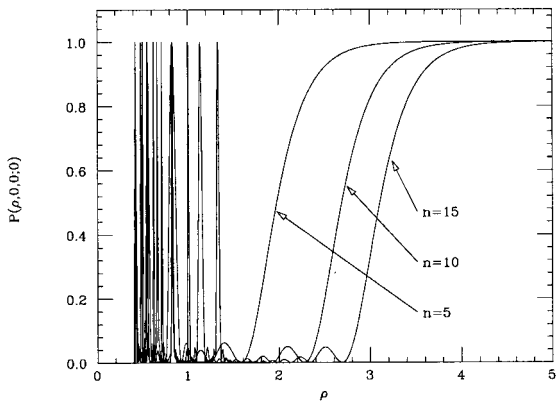

FIG. 7. Isolation probabilities of the $l=0$ state $P(\rho,0,0;0)$ for $n=5$, 10, and 15 as a function of ρ.

is presented. Roughly speaking, $\Delta l=1$ transition is favored for a given l and m and a smaller l is favored for given Δl and m. The comparison with the standard Leon-Bethe model and Borie-Leon model are described in the following sections.

4. Comparison with the past two models

a. Leon-Bethe model. Leon and Bethe [3] considered only the $m=0$ states because their discussion was concentrated on the transition $|1\leqslant l\leqslant n-1,\ m=0\rangle\rightarrow|l=0,\ m=0\rangle$ which is followed by the nuclear absorption. They introduced the *isolation probability* of $l=0$ state:

$$P(\rho,0,0;0)=\frac{1}{n^2}\left|\sum_{n_1=0}^{n-1}\exp\left[-in_1\frac{3\pi n}{v\mu}\frac{\zeta(\rho)}{\rho}\right]\right|^2, \quad (23)$$

where we have used $\langle n_1,\ m=0|l=0,\ m=0\rangle=1/\sqrt{n}$ which is independent of l and n_1. As a function of ρ, the oscillation becomes faster exponentially as ρ decreases as shown in Fig. 7 because of the ρ dependence of $\zeta(\rho)$ in Fig. 4. They assumed for simplicity that $P(\rho,0,0;0)$ is given by a step function :

$$P(\rho,0,0;0)=\begin{cases}1 & (\rho>\rho_S)\\ 1/n & (\rho\leqslant\rho_S).\end{cases} \quad (24)$$

After a collision with an impact parameter in the region $\rho\leqslant\rho_S$, the n states with $m=0$ are completely mixed up, which results in a uniform distribution among n states with $m=0$: $P(\rho,l,l';0)=1/n$ for any l and l'. ρ_S is the *effective impact parameter* for Stark mixing determined by their ''s-state mixing criterion''

$$\frac{\zeta(\rho_S)}{\rho_S}=\frac{v\mu}{2n^2} \quad (25)$$

which approximately satisfies $P(\rho_S,0,0;0)=0.1$ (see Ref. [3] for more details).

Stark mixing rate of $|1\leqslant l\leqslant n-1,\ m=0\rangle\rightarrow|l=0,\ m=0\rangle$ transition (averaged over initial l) is calculated as follows:

$$\begin{aligned}\frac{1}{n-1}\sum_{l=1}^{n-1}\Gamma^{\rm Stark}_{l\rightarrow l'=0;m=0}&=Nv2\pi\int_0^\infty\rho d\rho\frac{1}{n-1}\{1-P(\rho,0,0;0)\}\\&\simeq Nv\frac{\pi\rho_S^2}{n}.\end{aligned} \quad (26)$$

Noticing that the number of states in a given m is $n-|m|$, Eq. (26) can be extended for $m\neq0$ as

$$\Gamma^{\rm Stark}_{l\rightarrow l'\neq l;m}\simeq Nv\frac{\pi\rho_S^2}{n-|m|}. \quad (27)$$

b. Borie-Leon model. The cascade calculation incorporating l dependence of population distribution was made by Borie and Leon [4] to obtain hadronic atom x-ray yields as a function of the target density, with a very simple assumption for Stark mixing rate

$$\Gamma^{\rm Stark}_{l\rightarrow l+1}=k_{\rm STK}Nv\pi\rho_S^2, \quad (28)$$

$$\Gamma^{\rm Stark}_{l\rightarrow l-1}=k_{\rm STK}Nv\pi\rho_S^2\times\frac{2l-1}{2l+1}, \quad (29)$$

where $k_{\rm STK}$ is an arbitrary multiplying factor (putting $k_{\rm STK}$ as 1.5 to 2.0 reproduces the experimental x-ray yields well) and ρ_S is determined by the Leon-Bethe's criterion given in Eq. (25). The factor $(2l-1)/(2l+1)$ comes from the averaging over initial $2l+1$ substates of $-l\leqslant m\leqslant l$, where $|m|$ dependence of the Stark mixing approximately given by Eq. (27) is completely ignored.

In this model we ignore $\Delta l\geqslant2$ transitions

$$\Gamma^{\rm Stark}_{l\rightarrow l\pm\Delta l}=0 \quad \text{for } \Delta l\geqslant2. \quad (30)$$

However, it does not mean that we have merely neglected $\Delta l\geqslant2$ transitions in the Leon-Bethe model because the right-hand side of Eq. (29) is $\pi\rho_S^2$, which was $\pi\rho_S^2/n$ in Eq. (26) (see Fig. 6). The atom goes from the state with $1\leqslant l\leqslant n-2$ to $l'=l\pm1$ with the probability of $k_{\rm STK}\times[1+(2l-1)/(2l+1)](\geqslant1)$. Although it can reproduce the density dependence of experimental results by adjusting the free parameter $k_{\rm STK}$, Borie-Leon model involves such unnatural assumptions which were not assumed in the Leon-Bethe model.

The difference between the resultant Stark mixing rates with Borie-Leon model and the present calculation is obviously seen from Table I. Note that $|\Delta l|\geqslant2$ transitions are not at all negligible compared to $|\Delta l|=1$ transitions.

D. Stark mixing in the presence of nuclear interaction

In the preceding sections, we have neglected the effect of nuclear interaction. However, it plays an important role in Stark mixing because the strong interaction energy shift removes the degeneracy of n^2 states which is essential for the Stark mixing.

1. Interference of Stark mixing and nuclear interaction

First, we consider Stark mixing between n states with $m=0$ in the fixed field model, including nuclear interaction on the s-state. Note that some of the results by Leon and Bethe [3] are incorrectly given probably due to typographical error, although the discussion in this section follows them.

Together with the nuclear interaction (the vacuum polarization and the finite size effect are also included in its real part), the matrix element of Hamiltonian in the Stark representation is written as

$$\begin{aligned}\langle n_1|H|n_1'\rangle &= \langle n_1|V^{\text{Stark}}|n_1'\rangle + \langle n_1|V^{\text{nuclear}}|n_1'\rangle \\ &= 3En\left(n_1 - \frac{n-1}{2}\right)\delta_{n_1,n_1'} + \frac{\delta E_{l=0}}{n} \qquad (31)\end{aligned}$$

where $\delta E_{l=0}$ is the complex energy shift for the s state and we have used $\langle l=0|n_1\rangle = 1/\sqrt{n}$. If we set the complex energy eigenvalue as λ and introduce parameters according to Leon and Bethe [3]

$$\beta = \frac{\lambda}{3En}, \qquad (32)$$

$$\gamma = i\left(\frac{\delta E_{l=0}}{n}\right) \Big/ \left(\frac{3}{2}En\right) = \frac{2i\,\delta E_{l=0}}{3En^2}, \qquad (33)$$

and

$$a_{n_1} = \frac{2i}{\gamma}\left(n_1 - \frac{n-1}{2} - \beta\right), \qquad (34)$$

the matrix can be diagonalized by solving the characteristic equation

$$\begin{aligned}|H-\lambda U| &= 3En\frac{\gamma}{2i}|1 + a_{n_1}\delta_{n_1,n_1'}| \\ &= 3En\frac{\gamma}{2i}a_0\cdots a_{n-1}\left(1 + \frac{1}{a_0} + \cdots + \frac{1}{a_{n-1}}\right) \\ &= 0, \qquad (35)\end{aligned}$$

where the last term leads to a characteristic equation for β:

$$\sum_{n_1=0}^{n-1}\frac{1}{n_1 - [(n-1)/2] - \beta} = \frac{2}{i\gamma}. \qquad (36)$$

As for the set of the roots β_i $(i=1,\ldots,n)$, substituting Eq. (34) into Eq. (35) and rearranging with respect to β, we obtain from the coefficient of β^{n-1}

$$\sum_{i=1}^{n}\beta_i = -\frac{in\gamma}{2}. \qquad (37)$$

For small $|\gamma|$ (Stark splitting $\gg$ energy shift), the eigenvalues are

$$\beta \sim n_1 - \frac{n-1}{2} - \frac{i\gamma}{2}, \qquad (38)$$

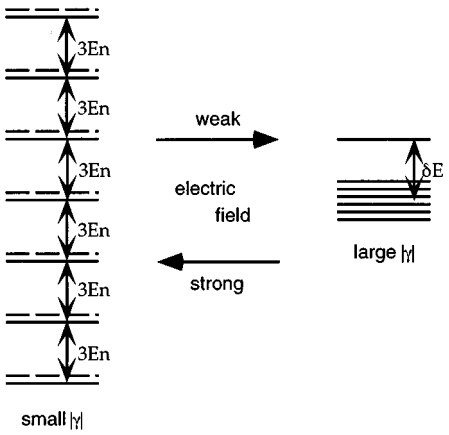

FIG. 8. Interference of Stark splitting and nuclear interaction in the two extreme of small $|\gamma|$ and large $|\gamma|$.

$$\lambda \sim 3En\left(n_1 - \frac{n-1}{2}\right) + \frac{\delta E_{l=0}}{n}, \qquad (39)$$

with $n_1 = 0,\ldots,n-1$, which are slightly perturbed from their values without $\delta E_{l=0}$. This means that n eigenstates are uniformly influenced by the $1/n$ of the s-state interaction.

At the limit of large $|\gamma|$ (Stark splitting $\ll$ energy shift), one of the β eigenvalues is large in absolute magnitude as

$$\begin{aligned}\frac{2}{i\gamma} &= \sum_{n_1=0}^{n-1}\frac{1}{n_1 - [(n-1)/2] - \beta_S} \\ &\to -\frac{n}{\beta_S} - \frac{1}{\beta_S{}^3}\frac{n(n^2-1)}{12} + \cdots (|\beta_S| \to \infty), \qquad (40)\end{aligned}$$

which results in

$$\beta_S \sim -\frac{in\gamma}{2}\left(1 - \frac{n^2-1}{3n^2\gamma^2}\right), \qquad (41)$$

$$\lambda_S \sim \delta E_{l=0}\left(1 - \frac{n^2-1}{3n^2\gamma^2}\right). \qquad (42)$$

The corresponding eigenstate is a slightly perturbed s state. The remaining $n-1$ eigenvalues lie close to the real axis and the eigenstates are linear combinations of the $l>0$ states. We have the *average energy shift* of these states other than the slightly perturbed s state using Eq. (37)

$$\overline{\beta_{l>0}} \sim \frac{1}{n-1}\left(\sum_{i=1}^{n}\beta_i - \beta_S\right) = -i\frac{n+1}{6n\gamma} \qquad (43)$$

$$\overline{\lambda_{l>0}} = 3En\overline{\beta_{l>0}} \sim -\frac{n+1}{12}\frac{(3En)^2}{\delta E_{l=0}}. \qquad (44)$$

Hence, the slightly perturbed s state is isolated and the strong interaction effects on the other states are very small at this limit. Figure 8 shows these two extreme cases diagrammatically.

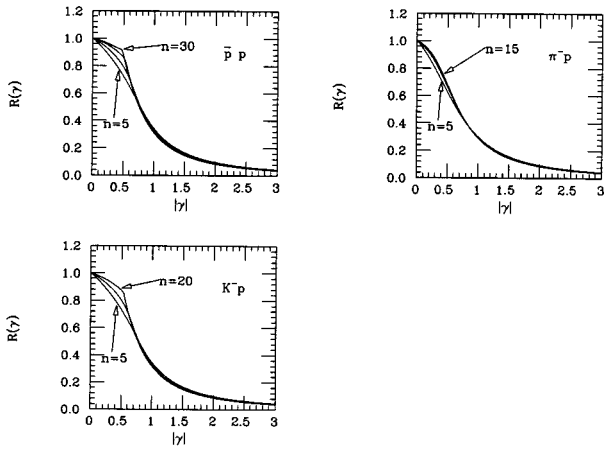

FIG. 9. Degree of Stark mixing $\mathcal{R}(\gamma)$ for antiprotonic ($n=5,10,20,30$), pionic ($n=5,10,15$), and kaonic ($n=5,10,20$) atoms.

2. Suppression of Stark transition from and to s states

We parametrize the degree of Stark mixing by the strong interaction effect on the states other than the slightly perturbed s states. We introduce a measure of the strength of the Stark mixing according to Leon and Bethe [3]:

$$\mathcal{R}=\frac{\mathrm{Im}\overline{\lambda_{l>0}}}{\mathrm{Im}(\delta E_{l=0}/n)}=-\frac{2\mathrm{Im}\overline{\beta_{l>0}}}{\mathrm{Re}\gamma}, \tag{45}$$

which is at two extremes in the previous section

$$\mathcal{R}(\gamma)\rightarrow 1 \quad (|\gamma|\rightarrow 0), \tag{46}$$

$$\mathcal{R}(\gamma)\rightarrow \frac{n+1}{3n}\frac{1}{|\gamma|^2} \quad (|\gamma|\rightarrow\infty). \tag{47}$$

In the region of $|\gamma|\sim 1$, the behavior of $\mathcal{R}(\gamma)$ depends on n and the phase of γ (i.e., $\delta E_{l=0}$). Figure 9 shows $\mathcal{R}(\gamma)$ calculated with the numerical solutions of Eq. (36) for antiprotonic, pionic, and kaonic hydrogen atoms.

Borie and Leon [4] incorporated the suppression of Stark mixing by replacing ρ_S to smaller effective impact parameters defined with $\mathcal{R}$, but the l, Δl, and m dependence are not taken into account at all. We treat it in a more realistic manner using the same $\mathcal{R}$.

Since γ involves the reciprocal of the electric field strength, $\mathcal{R}$ is a function of the distance from the target hydrogen nucleus. We assume the rate of the Stark mixing from and to the s state at a distance R from the hydrogen nucleus are suppressed as

$$\Gamma^{\mathrm{Stark}}_{l=0\leftrightarrow l'\neq 0}(R)\rightarrow\Gamma^{\mathrm{Stark}}_{l=0\leftrightarrow l'\neq 0}(R)\mathcal{R}(R). \tag{48}$$

This brings about the modification only for $P(\rho,0,l'\neq 0;0)$ and $P(\rho,l\neq 0,0;0)$ in the preceding calculation as

$$\langle l|V^{\mathrm{Stark}}(R)|l'\rangle\rightarrow\langle l|V^{\mathrm{Stark}}(R)|l'\rangle\sqrt{\mathcal{R}(R)} \tag{49}$$

so that $\zeta(\rho)$ defined in Eq. (20) is replaced by

$$\zeta(\rho)\rightarrow\zeta'(\rho)$$
$$=\frac{1}{\pi}\int_{-\pi/2}^{\pi/2}e^{-2\rho\sec\theta}\times(1+2\rho\sec\theta+2\rho^2\sec^2\theta)\sqrt{\mathcal{R}(\rho\sec\theta)}d\theta. \tag{50}$$

Note that $|\gamma|$ is minimum at $R=\rho$ where $\mathcal{R}(R)$ is maximum. The hadronic hydrogen atom feels electric field strong enough to cause Stark mixing only if ρ is small enough. It should be pointed out that in the small electric field limit ($|\gamma|\rightarrow\infty$),

$$\Gamma^{\mathrm{Stark}}_{l=0\leftrightarrow l'\neq 0}\propto\frac{1}{|\delta E|^2} \tag{51}$$

holds as expected from perturbation theory.

III. NUMERICAL RESULTS AND DISCUSSION

A. Antiprotonic hydrogen atoms

Since the antiprotonic hydrogen atom is the most extensively studied among the hadronic hydrogen atoms, we shall use it as a test case of the cascade model. The shift and absorption width of $1s$ state are well determined from the direct measurement of the energy of $K_\alpha(2p\rightarrow 1s)$ x rays [10–14] and the absorption width of $2p$ state is also well determined from the relative intensity [10,13,14]

$$Y=\frac{K_\alpha\ \text{yield}}{\Sigma_i L_i\text{yield}}=\frac{\Gamma^{\mathrm{rad}}_{2p\rightarrow 1s}}{\Gamma^{\mathrm{rad}}_{2p\rightarrow 1s}+\Gamma^{\mathrm{nuclear}}_{2p}} \tag{52}$$

where $\Gamma^{\mathrm{rad}}_{2p\rightarrow 1s}$ is the radiative width given in Eq. (3). We have used the latest values [14] which are consistent with the preceding experiments:

$$\mathrm{Re}\delta E_{1s}=\epsilon^{\mathrm{nuclear}}_{1s}+\epsilon^{\text{vacuum polarization}}_{1s}+\epsilon^{\text{finite size}}_{1s} \tag{53}$$
$$=-730(\text{repulsive})+41.8-3.2=-691\ \text{eV}, \tag{54}$$
$$\mathrm{Im}\delta E_{1s}=\Gamma^{\mathrm{nuclear}}_{1s}/2=561\ \text{eV}, \tag{55}$$
$$\Gamma^{\mathrm{nuclear}}_{2p}=34.0\ \text{meV}, \tag{56}$$

where $\epsilon^{\text{vacuum polarization}}_{1s}$ and $\epsilon^{\text{finite size}}_{1s}$ are given in Ref. [15]. Note that the sign of the energy shift ϵ_{1s} is defined so that positive is attractive.

1. Initial kinetic energy dependence

The results on the density dependence of K and L x rays yields are shown in Fig. 10 and Fig. 11 together with the experimental data. The only parameter is the initial kinetic energy T of the antiprotonic hydrogen atom and we have performed calculations for $T=0.5$ eV, 1.0 eV, and 2.0 eV. Although the data at low density region by PS175 group [13,14] are somewhat underestimated, the model seems to explain the experimental results, especially at medium density region.

2. Comparison with Borie-Leon model

We can also compare the results with those obtained using the original code of Borie and Leon [4] which has the

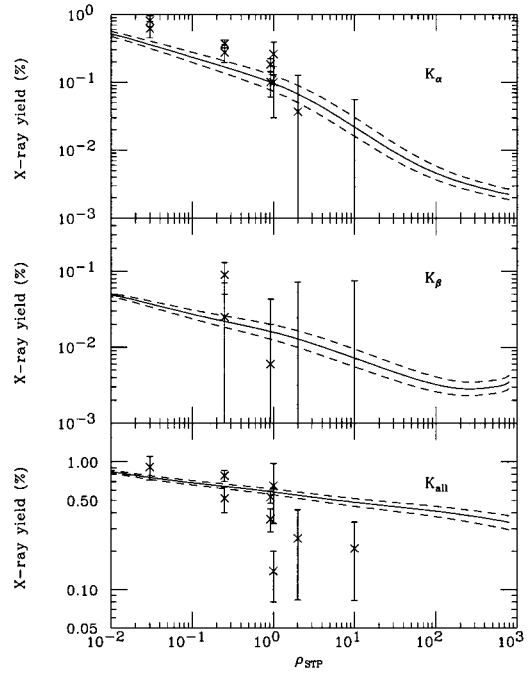

FIG. 10. Density dependence of K x-ray yields for antiprotonic hydrogen atoms. The lines are the numerical results for $T=0.5$ eV (top), 1.0 eV (middle), and 2.0 eV (bottom). The points with error bars are the experimental results from Refs. [10,12–14,16,17]. 1 ρ_{STP} is the target density at standard temperature (273 K) and pressure (1 atm).

arbitrary free parameter k_{STK} for multiplying Stark mixing rate uniformly as given in Eq. (29). We set k_{STK} to be 1.0, 1.5, and 2.0 and fixed T at 1.0 eV. The results are shown in Fig. 12 and Fig. 13.

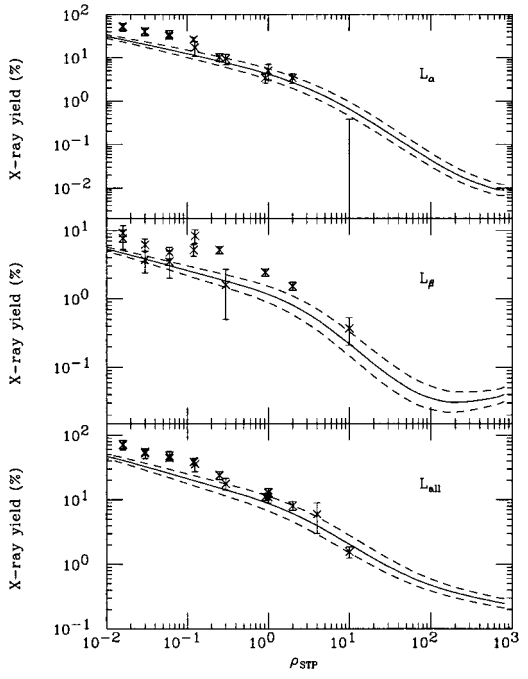

FIG. 11. Density dependence of L x-ray yields for antiprotonic hydrogen atoms. The lines are the numerical results for $T=0.5$ eV (top), 1.0 eV (middle), and 2.0 eV (bottom). The points with error bars are the experimental results from Refs. [10,13,14,16–18].

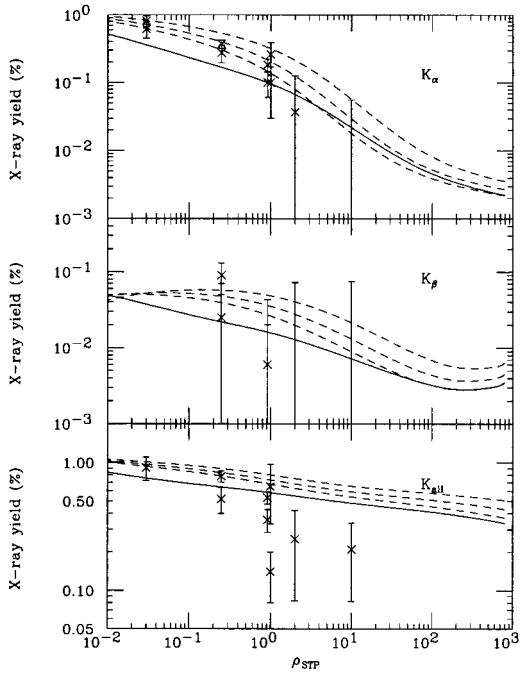

FIG. 12. Density dependence of K x-ray yields for antiprotonic hydrogen atoms. The solid lines are the present results and the dashed lines are obtained from the Borie-Leon model with $k_{STK}=1.0$ (top), 1.5 (middle), and 2.0 (bottom). The initial kinetic energy is fixed at $T=1.0$ eV.

The present model results in comparable or lower x-ray yields, or in other words, comparable or stronger Stark mixing rates than even in the $k_{STK}=2.0$ case of the Borie-Leon model in the most of the density region; we do not need to introduce an ambiguous factor k_{STK} to increase the Stark mixing rates any more. Apparently, the density dependence of x-ray yields in the present results cannot be reproduced by just adjusting a single parameter k_{STK} of Borie-Leon model.

It also should be noted that the present results agree with the experimental data less well than Borie-Leon model with $k_{STK}=2.0$ in the lower density region, where the effect of Stark mixing is relatively small. This may be attributed to the other physics as we will discuss later.

3. Other ambiguities

a. Initial population distribution. The statistical initial population distribution of $P(l)\propto(2l+1)$ at $n\sim\sqrt{\mu}$ is merely an assumption which can be justfied by the idea that the strong Stark mixing at higher n states makes angular momentum states far from energy eigenstates. We checked this picture by setting $P(l)\propto(2l+1)e^{\alpha l}$ and varying α from -0.2 to 0.2. The results showed that increasing α makes essentially no change and decreasing α reduces the yields slightly (by the order of 1% at the maximum). As a whole, these changes are negligible compared to other ambiguities such as the initial kinetic energy of the hadronic atoms.

b. Experimental errors of fixed parameters. Although we have used $\epsilon_{1s}^{nuclear}$, $\Gamma_{1s}^{nuclear}$, and $\Gamma_{2p}^{nuclear}$ as fixed parameters, they have experimental errors [14]. We evaluated the effect of them by changing these values within the range of error bars. The resultant K x-ray yields are affected by about 10%

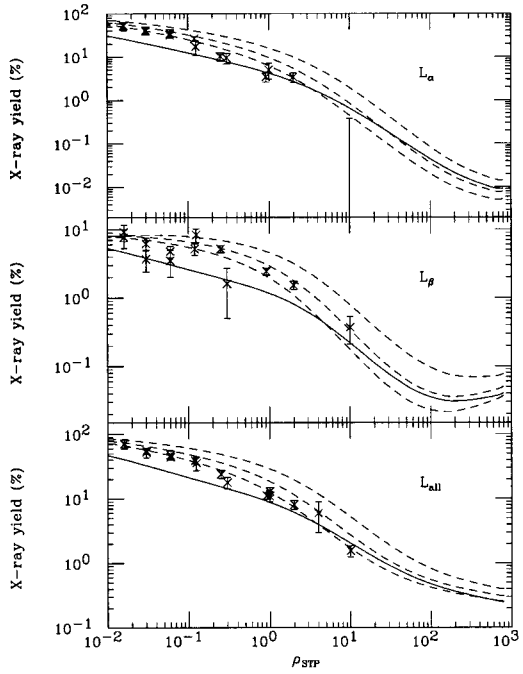

FIG. 13. Density dependence of L x-ray yields for antiprotonic hydrogen atoms. The solid lines are the present results and the dashed lines are obtained from the Borie-Leon model with $k_{\mathrm{STK}}=1.0$ (top), 1.5 (middle), and 2.0 (bottom). The initial kinetic energy is fixed at $T=1.0$ eV.

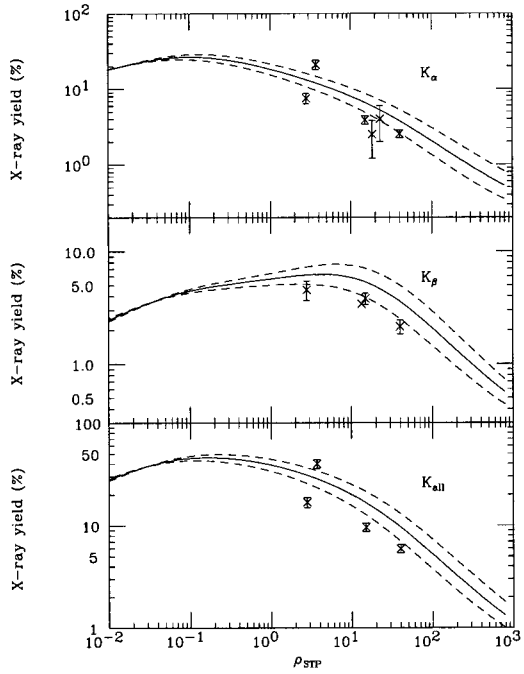

FIG. 14. Density dependence of K x-ray yields for pionic hydrogen atoms. The lines are the numerical results for $T=0.5$ eV (top), 1.0 eV (middle), and 2.0 eV (bottom). The points with error bars are the experimental results from Refs. [19,20,22–24].

but L x-ray yields are little affected; these changes are also negligible compared to those by the initial kinetic energy.

c. Molecular dissociation cross section. Γ^{mol} is conventionally taken to be the size of the hadronic atom with a classical Bohr radius as in Eq. (1). To evaluate the ambiguity caused by this simple assumption, the calculations are performed with changing the cross section by a factor of 0.5 and 2.0. The resultant changes are also about 10% at the maximum, which is smaller than the ambiguity due to initial kinetic energy.

B. Pionic hydrogen atoms

The experimental data on pionic hydrogen atoms is rather limited compared to antiprotonic hydrogen atoms because of their low binding energy. The crystal spectrometer enabled us to determine the shift and width of $1s$ state of pionic hydrogen atoms by the measurements of $K_\alpha(2p\rightarrow 1s)$ [19,20] and recently $K_\beta(3p\rightarrow 1s)$ [21,22] x-rays. We have used the latest values [22] which are consistent with the preceding experiment [21]

$$\mathrm{Re}\delta E_{1s}=\epsilon_{1s}^{\mathrm{nuclear}}+\epsilon_{1s}^{\text{vacuum polarization}}+\epsilon_{1s}^{\text{finite size}} \tag{57}$$

$$=7.13(\text{attractive})+3.23-0.1=10.3\ \text{eV}, \tag{58}$$

$$\mathrm{Im}\delta E_{1s}=\Gamma_{1s}^{\mathrm{nuclear}}/2=0.49\ \ \text{eV}. \tag{59}$$

The resultant x-ray yields are little affected by the experimental errors of them. However, since no L x ray is observed, we have no information on the nuclear absorption width of $2p$ state $\Gamma_{2p}^{\mathrm{nuclear}}$. We regard it as another unknown parameter.

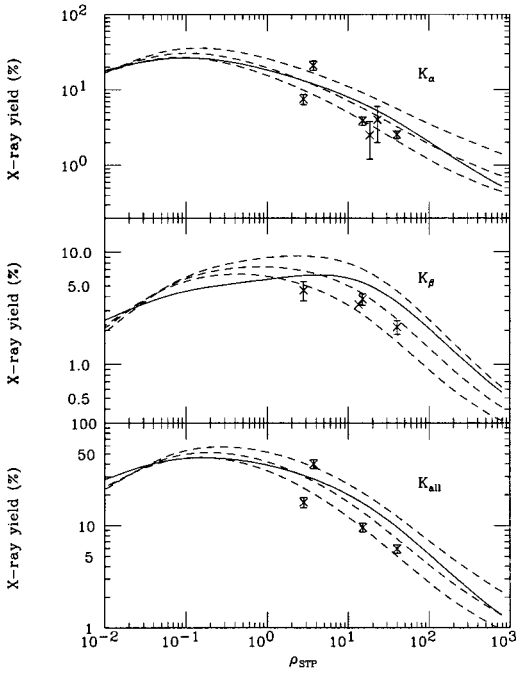

FIG. 15. Density dependence of K x-ray yields for pionic hydrogen atoms. The solid lines are the present results and the dashed lines are obtained from the Borie-Leon model with $k_{\mathrm{STK}}=1.0$ (top), 1.5 (middle), and 2.0 (bottom). In both models, $T=1.0$ eV and $\Gamma_{2p}^{\mathrm{nuclear}}=0$ meV.

1. Initial kinetic energy dependence

We first evaluate the initial kinetic energy dependence of the x-ray yields with $\Gamma_{2p}^{\text{nuclear}}$ set at zero. The initial kinetic energy is taken to be $T=0.5$ eV, 1.0 eV, and 2.0 eV. The results are shown in Fig. 14 together with the experimental data on the K x-ray yields. Note that increasing $\Gamma_{2p}^{\text{nuclear}}$ makes the x-ray yields much smaller as we will see later.

2. Comparison with Borie-Leon model

We again compare the results with those obtained using the original code of Borie and Leon [4]. We varied k_{STK} as 1.0, 1.5, and 2.0, with $T=1.0$ eV and $\Gamma_{2p}^{\text{nuclear}}=0$ meV. The results are shown in Fig. 15 where the difference between the present result and $k_{\text{STK}}=1.0$ is not so large as in the antiprotonic hydrogen case, but still the present model always results in lower x-ray yields than the Borie-Leon model with $k_{\text{STK}}=1.0$.

3. Influence of introducing $\Gamma_{2p}^{\text{nuclear}}$

We have ignored $\Gamma_{2p}^{\text{nuclear}}$ just because there exists no data on it. But some of the fraction in p state may well be captured to the nucleus, and hence the p state has a finite absorption width.

We here regard $\Gamma_{2p}^{\text{nuclear}}$ as a parameter and its effect on the results is shown in Fig. 16. Although ambiguity due to the initial kinetic energy exists, $\Gamma_{2p}^{\text{nuclear}}$ is estimated roughly not to be larger than 0.1 meV and $\Gamma_{2p}^{\text{nuclear}}=0.5$ meV is highly improbable.

C. Kaonic hydrogen atoms

At present, three experimental results are reported on the measurement of the strong interaction shift and width of K_α x rays from kaonic hydrogen atoms, but all of them suffer from very poor statistics [25–27]. The results are inconsistent with one another as shown in Table II.

What is more confusing, the sign of the shifts is opposite to that deduced from the extrapolation of scattering data to the low energy limit with Deser's formula [28,29]

$$\epsilon_{1s}^{\text{nuclear}}+i\frac{\Gamma_{1s}^{\text{nuclear}}}{2}=2\alpha^3\mu^2 a=412(\text{eV/fm})a, \tag{60}$$

where a is the scattering length obtained from the analysis of low energy scattering data [30–37]. The results are almost consistent except for Conboy [36] as shown in Table III, which are within the range of $-400\ \text{eV}<\epsilon_{1s}^{\text{nuclear}}<-300$ eV and $500\ \text{eV}<\Gamma_{1s}^{\text{nuclear}}<600$ eV.

We have used the approximate central value

$$\text{Re}\,\delta E_{1s}=\epsilon_{1s}^{\text{nuclear}}+\epsilon_{1s}^{\text{vacuum polarization}} \tag{61}$$

$$=-350(\text{repulsive})+25=-325\ \text{eV}, \tag{62}$$

$$\text{Im}\,\delta E_{1s}=\Gamma_{1s}^{\text{nuclear}}/2=275\ \text{eV}, \tag{63}$$

where $\epsilon_{1s}^{\text{vacuum polarization}}$ is given in Ref. [4]. Changing $\Gamma_{1s}^{\text{nuclear}}$ by ± 50 eV does not make any significant effect on the x-ray yields.

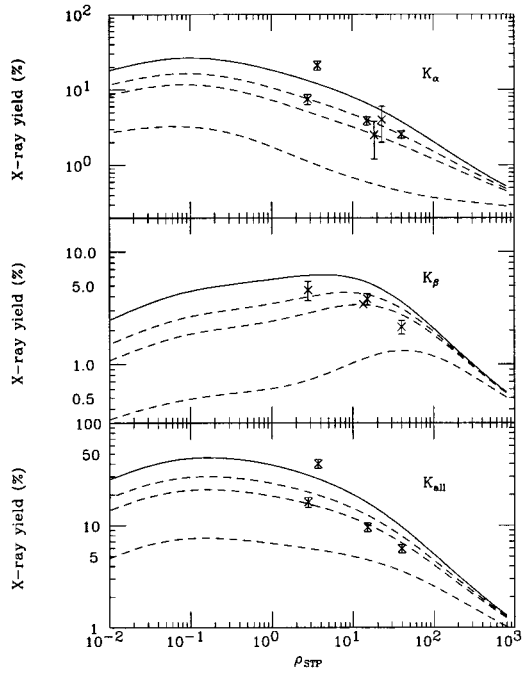

FIG. 16. Density dependence of K x-ray yields for pionic hydrogen atoms. The solid lines are the results without $\Gamma_{2p}^{\text{nuclear}}$ and the dashed lines are obtained with $\Gamma_{2p}^{\text{nuclear}}=0.05$ (top), 0.1 (middle), and 0.5 meV (bottom). In all cases, the initial kinetic energy T is fixed at 1.0 eV.

1. Initial kinetic energy dependence

We again evaluate the initial kinetic energy dependence of the results with $\Gamma_{2p}^{\text{nuclear}}$ set at zero for a while. The initial kinetic energy is varied as $T=0.5$ eV, 1.0 eV, and 2.0 eV. The results are shown in Fig. 17 and Fig. 18 together with the experimental data on K x-ray yields with liquid hydrogen targets. Note that increasing $\Gamma_{2p}^{\text{nuclear}}$ makes the x-ray yields much smaller as we will see later.

2. Comparison with Borie-Leon model

We compare the results with those obtained by the original code of Borie and Leon [4]. We varied k_{STK} as 1.0, 1.5, and 2.0, with $T=1.0$ eV and $\Gamma_{2p}^{\text{nuclear}}=0$ meV. The results are shown in Fig. 19 and Fig. 20. Again, the present model gives smaller x-ray yields than Borie-Leon model with $k_{\text{STK}}=2.0$ at high density.

3. Influence of introducing $\Gamma_{2p}^{\text{nuclear}}$

We again introduce $\Gamma_{2p}^{\text{nuclear}}$ which has not been measured experimentally. Its effect on the results are shown in Fig. 21 and Fig. 22.

TABLE II. The reported experimental data on shift and width of $1s$ state of kaonic hydrogen atoms.

Authors	$\epsilon_{1s}^{\text{nuclear}}$ (eV)	$\Gamma_{1s}^{\text{nuclear}}$ (eV)
Davies *et al.* [25]	$+40\pm60$	0^{+230}_{-0}
Izycki *et al.* [26]	$+270\pm80$	560 ± 260
Bird *et al.* [27]	$+193\pm60$	80^{+220}_{-80}

TABLE III. The prediction on shift and width of $1s$ state of kaonic hydrogen atoms from the analyses of scattering data.

Authors	Scattering length a (fm)	$\epsilon_{1s}^{\text{nuclear}}$ (eV)	$\Gamma_{1s}^{\text{nuclear}}$ (eV)
Kim [30]	$-0.87+i0.70$	-358	576
Martin and Ross [31]	$-0.91+i0.66$	-375	544
Chao *et al.* [32]	$-0.87+i0.70$	-358	576
Kumar and Nogami [33]	$-0.76+i0.72$	-313	594
Martin [34]	$-0.67+i0.64$	-276	528
Dalitz *et al.* [35]	$-0.73+i0.64$	-301	528
Conboy [36]	$-0.42+i0.75$	-171	614
Tanaka and Suzuki [37]	$-1.03+i0.75$	-424	618

If we believe in the yields reported in three experiments with liquid hydrogen targets, $\Gamma_{2p}^{\text{nuclear}}$ would be estimated to be between 1.0 meV and 10.0 meV. But the preliminary experimental result with 7 ρ_{STP} gaseous hydrogen target [38] by E228 group at KEK-PS [39] suggests a rather smaller $\Gamma_{2p}^{\text{nuclear}}$ of about 0.5 meV to 1.0 meV. The experimental results with gaseous and liquid targets cannot be explained at a time with a single value of $\Gamma_{2p}^{\text{nuclear}}$.

IV. DISCUSSION

We here point out some of the possibilities for a further refinement of the model. The disagreement between the present results and the experimental data, especially in the low density region for antiprotonic hydrogen atoms, may be attributed to these physics which are not incorporated in the model.

We assumed a uniform distribution of $2l+1$ substates with a given l, which corresponds to infinite $\Delta m=\pm 1$ transition rates. But obviously this is not the case. If we consider finite $\Delta m=\pm 1$ transition rates instead, population of the states with $m=0$, from which nuclear absorption occurs, are not fed so fast as in the uniform distribution assumption. Thus the nuclear absorption rate at high n states is expected to be somewhat decreased and the resultant x-ray yields are increased.

Throughout this paper, we have assumed the initial kinetic energy of the hadronic hydrogen atom is represented by a single avaraged energy of about 1 eV, which is expected from the molecular dissociation process. But actually there is a distribution of the energies. The shape of time-of-flight spectra of neutrons from the reaction $\pi^- p \to \pi^0 n$ in a recent measurement of the mass difference $m_{\pi^-}-m_{\pi^0}$ implies that a half of the pionic atoms are distributed around 1 eV, but

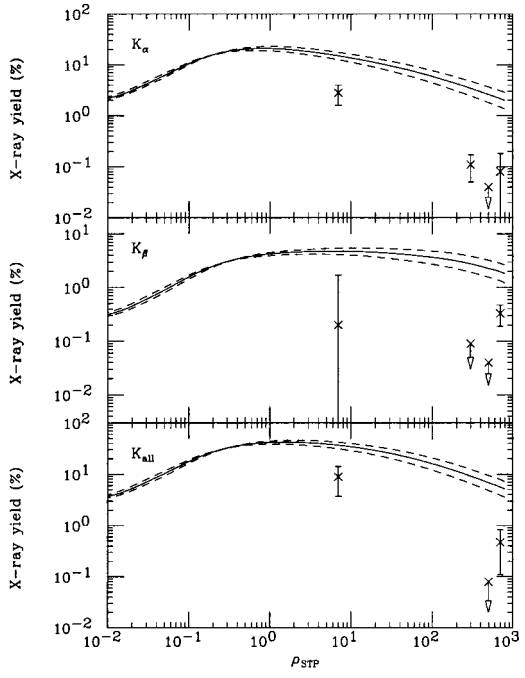

FIG. 17. Density dependence of K x-ray yields for kaonic hydrogen atoms. The lines are the numerical results for $T=0.5$ eV (top at high density), 1.0 eV (middle), and 2.0 eV (bottom). The three data points at 790 ρ_{STP} (liquid target) from Refs. [25–27] are slightly moved to the left-hand side to make it easy to see. A data point with an error bar at 7 ρ_{STP} is a preliminary result of KEK-PS E228 experiment [38].

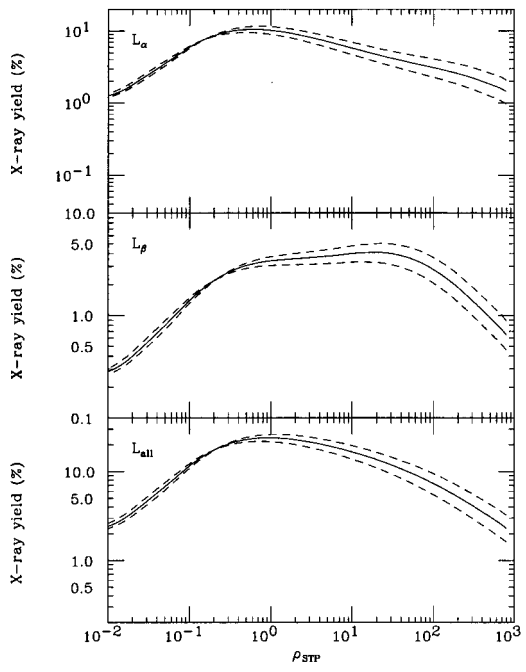

FIG. 18. Density dependence of L x-ray yields for kaonic hydrogen atoms. The lines are the numerical results for $T=0.5$ eV (top at high density), 1.0 eV (middle), and 2.0 eV (bottom).

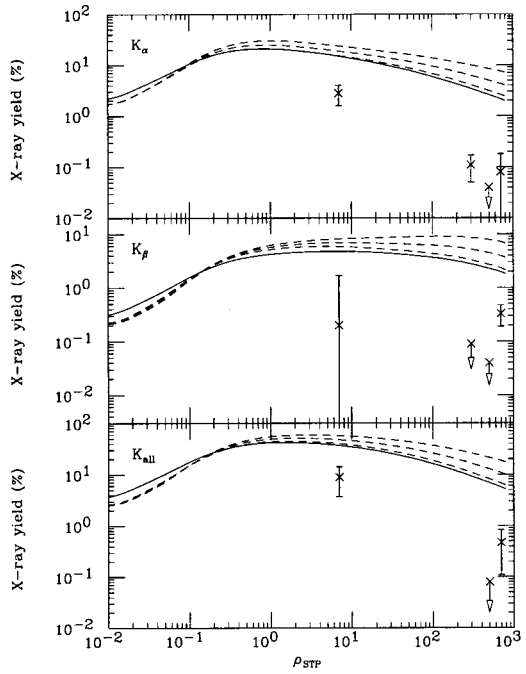

FIG. 19. Density dependence of K x-ray yields for kaonic hydrogen atoms. The solid lines are the present results and the dashed lines are obtained from the Borie-Leon model with $k_{\mathrm{STK}}=1.0$ (top), 1.5 (middle), and 2.0 (bottom). In both models, $T=1.0$ eV and $\Gamma_{2p}^{\mathrm{nuclear}}=0$ meV.

the rest extends up to about 70 eV [40–42]. The most likely candidate for the origin of this higher energy component is Coulomb deexcitation process, or in other words, Stark transition to the states with lower n [43]; the hadronic hydrogen

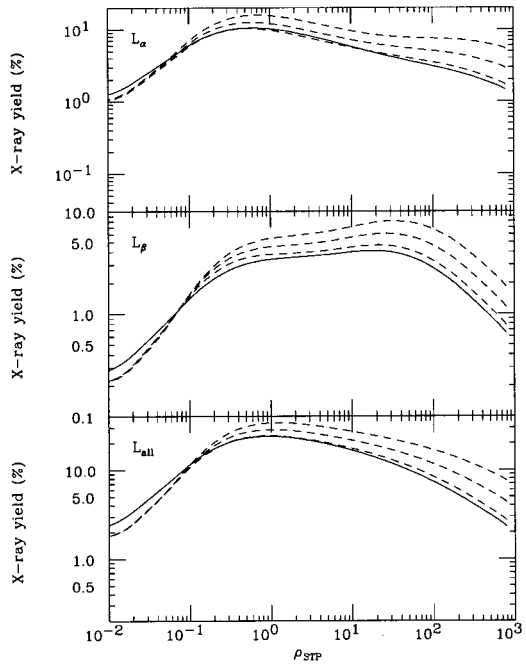

FIG. 20. Density dependence of L x-ray yields for kaonic hydrogen atoms. The solid lines are the present results and the dashed lines are obtained from the Borie-Leon model with $k_{\mathrm{STK}}=1.0$ (top), 1.5 (middle), and 2.0 (bottom). In both models, $T=1.0$ eV and $\Gamma_{2p}^{\mathrm{nuclear}}=0$ meV.

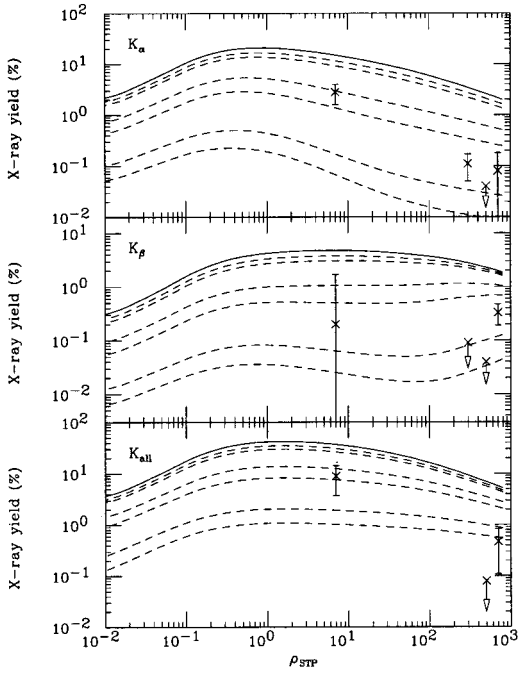

FIG. 21. Density dependence of K x-ray yields for kaonic hydrogen atoms. The solid lines are the results without $\Gamma_{2p}^{\mathrm{nuclear}}$ and the dashed lines are obtained with $\Gamma_{2p}^{\mathrm{nuclear}}=0.05$, 0.1, 0.5, 1.0, 5.0, and 10.0 meV (downwards). In all cases, the initial kinetic energy T is fixed at 1.0 eV.

atom is accelerated by the energy released with the transitions. In this point of view, the initial kinetic energy distribution may depend on the target density and thus the higher kinetic energy component is increased with the target density. But the quantitative estimation of this effect remains a complicated problem.

For antiprotonic hydrogen atoms, we have used the experimental value of $\Gamma_{2p}^{\mathrm{nuclear}}$, which is spin-averaged. In the original paper of Borie and Leon [4], comparison between the two cases are made in which the spin averaging is done before and after cascade calculation: cascade calculations are made with spin-averaged absorption width in the former and cascade calculations with different $\Gamma_{2p}^{\mathrm{nuclear}}$ for spin-triplet and spin-singlet are separately made and the x-ray yields are averaged in the latter. These two cases result in a difference of L x-ray yields by a factor of about 2, and the latter seems to be more appropriate because the cascade time is too short to allow any significant singlet-triplet transitions.

V. CONCLUSIONS

We extended the Leon-Bethe model to formulate Stark mixing rates in hadronic hydrogen atoms and its suppression due to nuclear interaction on s states. In the fixed field model with the impact parameter method, the full incorporation of l, Δl, and m with the initial kinetic energy $T\sim 1$ eV makes it possible to reproduce the reported x-ray intensities of pionic hydrogen atoms, but for antiprotonic hydrogen atoms, the agreement is less satisfactory especially in the low density region.

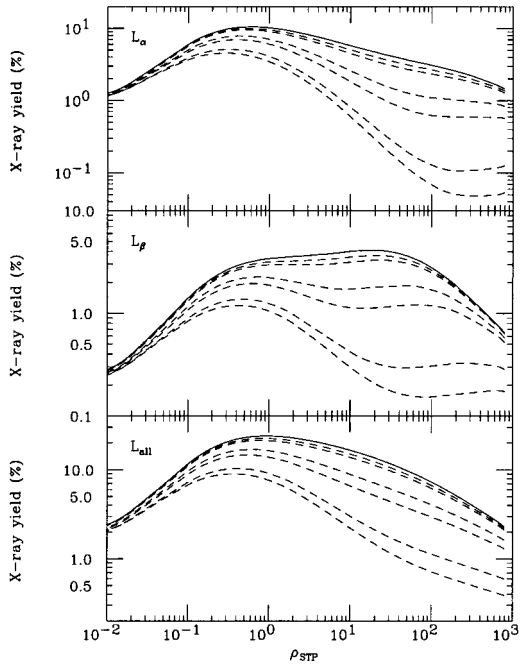

FIG. 22. Density dependence of L x-ray yields for kaonic hydrogen atoms. The solid lines are the results without $\Gamma_{2p}^{\text{nuclear}}$ and the dashed lines are obtained with $\Gamma_{2p}^{\text{nuclear}}=0.05$, 0.1, 0.5, 1.0, 5.0, and 10.0 meV (downwards). In all cases, the initial kinetic energy T is fixed at 1.0 eV.

The results were also compared with those of the Borie-Leon model, which has been widely used to understand the density dependence of x-ray yields from hadronic hydrogen atoms. We have eliminated the ambiguous parameter k_{STK}, which is needed in the model to enhance the Stark mixing rates. Our x-ray intensity results correspond to those obtained from the Borie-Leon model with $k_{\text{STK}}=1.5-2.0$ in the case of pionic hydrogen atoms, while our intensities are generally lower in the case of antiprotonic hydrogen atoms. The detailed aspects of our x-ray intensity results cannot be reproduced by merely changing the single parameter k_{STK}.

The ambiguity due to the change of the initial population distribution, the molecular dissociation cross section and the absorbtion widths within the experimental errors were confirmed for antiprotonic hydrogen atoms.

In pionic and kaonic hydrogen atoms, the results were shown to be very sensitive to the rate of nuclear absorption from p states. Since we do not have established data on it experimentally or theoretically, it prevents us from determining x-ray yields with only one parameter of initial kinetic energy T. But conversely, we can roughly estimate the order of $\Gamma_{2p}^{\text{nuclear}}$ from K x-ray yields without the L x-ray data which are much more difficult to obtain because of the low energy. As for pionic hydrogen atoms, $\Gamma_{2p}^{\text{nuclear}}$ is estimated to be not larger than about 0.1 meV. The reported K x-ray yields from kaonic hydrogen atoms with liquid hydrogen targets seem to imply that $\Gamma_{2p}^{\text{nuclear}}$ is between 1.0 meV and 10.0 meV, but it is inconsistent with the preliminary result with gaseous hydrogen target which suggests a smaller $\Gamma_{2p}^{\text{nuclear}}$ of about 0.5 meV to 1.0 meV.

ACKNOWLEDGMENTS

We are grateful to T. Koike for valuable discussions. Thanks are also due to Dr. M. Iwasaki, Dr. S. N. Nakamura, and T. M. Ito, who are the members of KEK-PS E228 group, for useful comments and the preliminary experimental result on K_α x-ray yield of kaonic hydrogen atoms.

[1] T. B. Day, G. A. Snow, and J. Sucher, Phys. Rev. Lett. **3**, 61 (1959).
[2] T. B. Day, G. A. Snow, and J. Sucher, Phys. Rev. **118**, 864 (1960).
[3] M. Leon and H. A. Bethe, Phys. Rev. **127**, 636 (1962).
[4] E. Borie and M. Leon, Phys. Rev. A **21**, 1460 (1980).
[5] T. Koike, T. Harada, and Y. Akaishi, Phys. Rev. C **53**, 79 (1996).
[6] C. J. Batty, Sov. J. Part. Nucl. **13**, 71 (1982).
[7] H. A. Bethe and E. E. Salpeter, *Quantum Mechanics of One- and Two-Electron Atoms* (Academic Press, New York, 1957).
[8] G. Reifenröther and E. Klempt, Nucl. Phys. **A503**, 885 (1989).
[9] G. Reifenröther and E. Klempt, Phys. Lett. B **248**, 250 (1990).
[10] C. A. Baker *et al.*, Nucl. Phys. **A483**, 631 (1988).
[11] M. Ziegler *et al.*, Phys. Lett. B **206**, 151 (1988).
[12] C. W. E. van Eijk *et al.*, Nucl. Phys. **A486**, 604 (1988).
[13] R. Bacher *et al.*, Z. Phys. A **334**, 93 (1989).
[14] K. Heitlinger *et al.*, Z. Phys. A **342**, 359 (1992).
[15] C. J. Batty, Rep. Prog. Phys. **52**, 1165 (1989).
[16] S. Ahmad *et al.*, Phys. Lett. **157B**, 333 (1985).
[17] U. Schaefer *et al.*, Nucl. Phys. **A495**, 451 (1989).
[18] E. G. Auld *et al.*, Phys. Lett. **77B**, 454 (1978).
[19] A. Forster *et al.*, Phys. Rev. C **28**, 2374 (1983).
[20] E. Bovet *et al.*, Phys. Lett. **153B**, 231 (1985).
[21] W. Beer *et al.*, Phys. Lett. B **261**, 16 (1991).
[22] D. Sigg *et al.*, Phys. Rev. Lett. **75**, 3245 (1995).
[23] J. Bailey *et al.*, Phys. Lett. **33B**, 639 (1970).
[24] A. J. Rusi El Hassani *et al.*, Z. Phys. A **351**, 113 (1995).
[25] J. D. Davies *et al.*, Phys. Lett. **83B**, 55 (1979).
[26] M. Izycki *et al.*, Z. Phys. A **297**, 11 (1980).
[27] P. M. Bird *et al.*, Nucl. Phys. **A404**, 482 (1983).
[28] S. Deser, M. L. Goldberger, K. Baumann, and W. Thirring, Phys. Rev. **96**, 774 (1954).
[29] T. L. Trueman, Nucl. Phys. **21**, 57 (1961).
[30] J. K. Kim, Ph.D. thesis, Columbia University, 1966.
[31] A. D. Martin and G. G. Ross, Nucl. Phys. **B16**, 479 (1970).
[32] Y.-A. Chao, R. W. Kreamer, D. W. Thomas, and B. R. Martin, Nucl. Phys. **B56**, 46 (1973).
[33] K. S. Kumar and Y. Nogami, Phys. Rev. D **21**, 1834 (1980).
[34] A. D. Martin, Nucl. Phys. **B179**, 33 (1981).
[35] R. H. Dalitz, J. McGinley, C. Belyea, and S. Anthony, Proceedings of the International Conference on Hypernuclear and

Kaon Physics, 201. (1982) (Report No. MPI H-1982-V20).
[36] J. E. Conboy, Report No. RAL-85-091 (1985).
[37] K. Tanaka and A. Suzuki, Phys. Rev. C **45**, 2068 (1992).
[38] S. N. Nakamura, Doctor thesis, University of Tokyo, 1995.
[39] M. Iwasaki *et al.*, Nucl. Phys. **A585**, 239c (1995).
[40] J. F. Crawford *et al.*, Phys. Rev. Lett. **56**, 1043 (1986).
[41] J. F. Crawford *et al.*, Phys. Lett. B **213**, 391 (1988).
[42] J. F. Crawford *et al.*, Phys. Rev. D **43**, 46 (1991).
[43] L. Bracci and G. Fiorentini, Nuovo Cimento A **43**, 9 (1977).